

Hydrologic processes at the urban residential scale

Q. Xiao,^{1*} E. G. McPherson,² J. R. Simpson² and S. L. Ustin¹

¹ Department of Land, Air, and Water Resources, University of California, Davis, CA 95616, USA

² Center for Urban Forest Research, USDA Forest Service, Pacific Southwest Research Station, c/o Dept. Plant Science, MS-6, One Shields Avenue, University of California, Davis, CA 95616, USA

Abstract:

In the face of increasing urbanization, there is growing interest in application of microscale hydrologic solutions to minimize storm runoff and conserve water at the source. In this study, a physically based numerical model was developed to understand hydrologic processes better at the urban residential scale and the interaction of these processes among different best management practices (BMPs). This model simulates hydrologic processes using an hourly interval for over a full year or for specific storm events. The model was applied to treatment and control single-family residential parcels in Los Angeles, California. Data collected from the control and treatment sites over 2 years were used to calibrate and validate the model. Annual storm runoff to the street was eliminated by 97% with installation of rain gutters, a driveway interceptor, and lawn retention basin. Evaluated individually, the driveway interceptor was the most effective BMP for storm runoff reduction (65%), followed by the rain gutter installation (28%), and lawn converted to retention basin (12%). An 11 m³ cistern did not substantially reduce runoff, but provided 9% of annual landscape irrigation demand. Simulated landscape irrigation water use was reduced 53% by increasing irrigation system efficiency, and adjusting application rates monthly based on plant water demand. The model showed that infiltration and surface runoff processes were particularly sensitive to the soil's physical properties and its effective depth. Replacing the existing loam soil with clay soil increased annual runoff discharge to the street by 63% when climate and landscape features remained unchanged. Copyright © 2006 John Wiley & Sons, Ltd.

KEY WORDS hydrologic processes; residential scale; best management practice; urban runoff reduction; landscape irrigation water use

Received 23 February 2006; Accepted 16 June 2006

INTRODUCTION

Population and economic growth have increased urbanization and conversion of rural areas into urban landscapes, and this has given rise to urban water resource management problems. The conversion of landscapes from pervious to impervious surfaces, including buildings, roads, and parking lots, has significantly changed the ecosystem hydrologic regime (Thom *et al.*, 2001). These changes reduce infiltration rates and surface water retention storage capacities, and increase runoff rates and total runoff water volumes. These factors are, in turn, associated with flooding that threatens people, wildlife, and property. In addition, surface runoff generated in an urban landscape is more likely to contribute to non-point-source pollution because it picks up a variety of pollutants (e.g. turf fertilizers, herbicides, insecticides, atmospheric dust, bird/animal faeces, asphalt-associated automotive discharges, bacteria and metals) (Stein and Tiefenthaler, 2005).

In California, polluted runoff, winter flooding and summer water shortages are critical problems that challenge planners and managers. For example, in Los Angeles, polluted runoff flows into local watersheds and then

into the scenic coastal recreation areas of Los Angeles' beaches and bays giving rise to health concerns from contaminated water (Haile, 1996; Haile *et al.*, 1999). Urban runoff is considered to be one of the largest sources of pollution to waterway and coastal areas (LACWS Management, 2000). Furthermore, as excess water brought by winter storms runs off from urban areas to the ocean, it also makes these water resources unavailable during the summer peak water-use period. Pollution transported through watersheds contributes to other ecological problems, such as bioaccumulation and eutrophication. Residential housing units and associated forms of landscaping and irrigation are a significant drain on the municipal potable water supply, contributing to local droughts and controversial demands for importing fresh water from elsewhere. Summer water deficits in Los Angeles result in the city importing 85% of its water (Gewe, 2003). Reducing storm water runoff hazards and providing sufficient water supplies are essential requirements for federal, state, and local water resource managers.

Traditionally, federal and local government agencies have addressed these problems through large-scale solutions. Pollutants have been managed through the National Pollution Discharge Elimination System permit programme, runoff through programmes such as the Standard Urban Storm Water Mitigation Plan, and

* Correspondence to: Q. Xiao, Department of Land, Air, and Water Resources, UC Davis, C/o Department of Plant Sciences, University of California, 1 Shields Avenue Davis, CA 95616, USA.
E-mail: qxiao@ucdavis.edu

the regulation of water supplies has relied on large-scale engineering projects, such as reservoir construction, riverbank augmentation, and cross-basin water transport. There has been little emphasis on conservation to supply urban water needs at the residential scale.

An alternative approach is using best management practices (BMPs) for source control at the parcel scale. Examples of the application of BMPs to urban landscapes included harvesting rainwater from roofs during rainy seasons, filtering and storing this water in onsite cisterns or rain barrels (a gravity-driven process), and using this stored water for landscape irrigation during the summer drought, thereby minimizing municipal water consumption (Braune and Wood, 1999). Capturing rainfall at the source can reduce the amount of runoff entering streets and rivers, reduce irrigation water demand, and conserve water. Runoff from driveways can be channelled by interceptors into lawn retention basins and drywells for filtering and infiltration, minimizing surface runoff and maximizing local pollution absorption. On-site residential storm runoff detention could be effective for hydrologic mitigation over a range of intermediate flows (Konrad and Burges, 2001). Retention/detention basins are created by grading, berming, and enhancing the sub-surface soil profile in lawn areas. Other pervious areas can incorporate mulching swales to maximize onsite rainwater infiltration and pollutant adsorption, and minimize surface runoff and non-point-source pollution. Vegetated swales function similarly as retention basins, but resemble a planting bed that can filter pollutants and also act as sites for green-waste recycling (Metro, 2002). Strategic tree planting has many virtues in the urban environment. The value of trees in a water-wise landscape is their ability to increase rainfall interception, increase soil permeability, and decrease ambient temperatures (Xiao and McPherson, 2002; Weng *et al.*, 2004; McPherson *et al.*, 2005).

The impact of BMPs on runoff and conservation of water resources is of growing interest as the efforts to reduce storm runoff and protect water quality increasingly focus on non-point pollution sources and the role of landscape irrigation water use within urban watersheds. BMPs can be developed that create a mini-reservoir system that retains runoff onsite and stores runoff for landscape irrigation. Policy makers are considering implementing this type of decentralized approach to urban watershed management, but they lack quantitative data on the effectiveness of different BMPs.

Well-established urban runoff models, such as the EPA Storm Water Management Model (Huber and Dickinson, 1988; Huber, 2001) and the Hydrological Simulation Program Fortran model (Bicknell *et al.*, 1997) have been developed for urban runoff management (Lee and Heaney, 2003) at different scales. However, little research has focused on the understanding of urban hydrologic processes at the parcel scale for both runoff and landscape irrigation water use because control strategies and management models have operated at much larger scales. Urban hydrologic models, such as those of Grimmond

et al. (1986) and Burian *et al.* (2002), focus on the water balance, but not on the effects of BMPs on urban hydrologic processes. Hydrologic processes at the watershed scale are sensitive to land use (Ha *et al.*, 2003). However, at the residential scale, land use is constant, but land cover changes frequently within a site. Science has yet to determine whether hydrologic processes are influenced in a similar way by BMPs applied at watershed and residential scales. This paper presents a physically based numerical model that simulates hydrologic processes at the residential scale for a full array of BMPs and land cover types.

OBJECTIVE

The overall goal of this study was to develop, calibrate, validate, and apply a physically based hydrologic model at the residential scale for simulating runoff to street and landscape irrigation water use. The model simulates hydrologic processes among different BMPs and land cover types in both long (annual) and short (storm event) time-frames. The following are the objectives of this study:

1. Measure hydrologic parameters at the residential parcel scale to increase our understanding of how BMPs will affect hydrologic processes.
2. Evaluate effectiveness of the BMPs installed in a residential site located in Los Angeles, California.
3. Determine sensitivity of runoff reduction and landscape irrigation water use to different BMPs.
4. Simulate effects of retrofitting the control site with BMPs. Specifically, how do BMPs affect runoff discharge and landscape irrigation water use?

METHODS

Study site

The study site is located in the Crenshaw district of south central Los Angeles, California (118°23'W, 33°56'N). Single-family housing units are the dominant form of urban construction and land cover in the Los Angeles basin (Condon *et al.*, 1999). The study site consists of adjacent treatment and control parcels on the 1800 block of West 50th Street, Los Angeles, California. The development is characteristic of single-family housing unit density, with the typical parcel sizes measuring 45.7 m × 15.2 m (150 ft × 50 ft). The garages are isolated from the houses and the paved driveways (Figure 1a). Both sites are located on well-developed loamy sand soil with a high infiltration rate and a deep active layer. The two parcels are used for evaluating BMPs and individual BMP's roles in runoff and landscape water use. The treatment site had six different BMPs (e.g. cistern, swale, rain gutter, lawn retention basin, driveway interceptor, and drywell) installed. Onsite BMP demonstrations of the treatment site were a part of

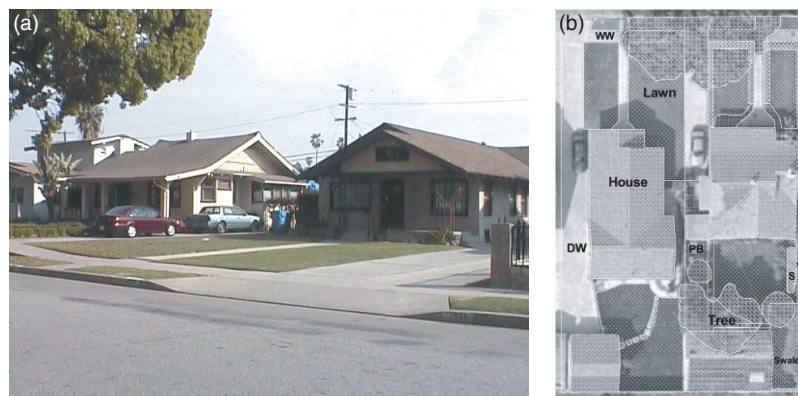


Figure 1. Study site. (a) View from northwest. Treatment (left) and control (right) sites are side by side with the same dimensions and shapes. (b) Land cover types were overlaid with high-resolution aerial photography for the treatment (left) and control (right) sites. Land covers include driveway (DW), paved walkway (WW), house, lawn, shrub (S), tree, swale, cistern (C), and planting bed (PB)

the Trans-Agency Resources for Environmental and Economic Sustainability education and outreach programme. These BMPs were designed to process, at a maximum capacity, a 50-year return storm event. Runoff from roof surfaces flowed to a cistern (13.6 m³; 3600 gal) and lawn retention basins (1715.8 ft²; 159.4 m²). The swale covers 486.6 ft² (45.2 m²). The driveway interceptor intercepts the runoff from the driveway and is connected to a 10.1 cm (4 in) diameter drywell (Condon *et al.*, 1999). No BMPs or landscape modifications were installed at the control site.

Field measurements

Field measurements were conducted at the treatment and control sites during January 2001 through to January 2003. The measurements included land covers, hydrologic processes, and microclimate data. Field measurement data were used for calibrating and validating the numerical model developed in this project.

Physical parameters of the sites were measured *in situ* by measuring parcel dimensions, structure dimensions (including roof slope and building materials), vegetation attributes (species and dimensions), and land cover (including ground surface areas and gradients of each land cover types). An analysis of the soil profile was conducted for 2 m downwards, coring with an auger and collecting samples at 25 cm intervals for laboratory analysis of soil texture, organic matter, and bulk density. Soil infiltration and percolation rates were also measured *in situ* used a double-ring infiltrometer (Sanders, 1998).

A geographic information system (GIS) database was created for the study site. The main layer in this database was land cover type. Land cover boundaries were determined based on both field measurements and high-resolution aerial photographic interpretation. The aerial photography was incorporated into the GIS layer and all land cover types were digitized for the study site (Figure 1b).

For each site, plastic bender boards (15.2 cm, or 6 in, tall) were installed on the property's boundaries and rubber strips (8.9 cm × 1.9 cm, or 3.5 in × 0.75 in) were installed on the walkway edges. These boundaries were to

prevent water from flowing across property boundaries. In the treatment site, the runoff discharge to the street occurred through the runoff collection and measurement system with sand filters, flow meters, and water outlet drainages. In the control site, the runoff from half of the roof drained directly to the driveway. The runoff from the driveway flowed directly into the street.

Hydrologic processes and microclimate data were measured for 2 years onsite by using a weather station (Campbell Scientific, Inc.), soil moisture sensors (CS615, Campbell Scientific, Inc.), and flow meters (FP5600, Omega Engineering, Inc.). The weather station measured air temperature, relative humidity, wind speed and direction, and precipitation. The flow meters measured irrigation water use and runoff flow to the street. Data were recorded in a data logger (CR10, Campbell Scientific, Inc.) every 10 min during the rainy season and 30 min during the dry season. Soil water contents were measured at depths of 15, 35, and 65 cm in the front and the backyards of both sites' turf grass areas.

Vegetation surface water storage capacities were measured in the laboratory for the 19 plant species found at the study site. The storage capacities were determined based on the weighing method of Wood *et al.* (1998).

Model

BMPs installed at the residential parcel create hydrologic sources and sinks that change urban hydrologic processes. For modelling hydrologic processes at a residential scale, we classified the parcel into different land cover types and different hydrologic sources and sinks. The secondary and tertiary land cover classes were further categorized (Table I).

Each land cover patch was treated as an individual modelling unit and flow destinations were specified. Hydrologic processes were modelled for each unit. Figure 2 shows the flow chart of the model structure. The model was designed to simulate hydrologic processes in both long (annual) and short (storm event) time-scales. For long-term simulation, it focused on both annual landscape irrigation water use and runoff to the street. For short-term simulation, the focus was on storm runoff to

Table I. Land cover classification

First class	Second class	Third class
Building	House Garage	
Paving surface	Pervious	Driving way Walk way
	Impervious	Driving way Walk way
Bare soil	Bare soil Planting bed	
Vegetation	Tree	Species
	Shrub	Species
	Lawn	Species
	Forb	
BMPs	Cistern	
	Driveway interceptor	
	Dry well	
	Retention/detention basin	Lawn Swale

the street and water storage in BMPs. The time interval was restricted by the input data. The time interval of the field-measured microclimate data varied from 10 to 30 min. However, since most meteorological data are recorded at 1 h intervals, the final time interval selected was 1 h. The model was calibrated and validated with field measurements data from the study site. A detailed description of the hydrologic processes and modelling procedures follows.

Precipitation and landscape irrigation. Precipitation and landscape irrigation are the primary driving forces of this model. Precipitation was not simulated but used the rainfall data as an explicit input data. Landscape irrigation provides additional water to satisfy plant water demand. Two different landscape irrigation strategies were used in this model to determine the timing and the amount of water to be applied. The first strategy was to use normal year monthly evapotranspiration ET derived from data measured by the California Irrigation Management Information System (CIMIS) to determine the amount of water that needs to be applied to balance ET. Irrigation interval, start time, and duration were specified explicitly. The irrigation controller can be changed in four different ways that correspond to current residential landscape irrigation practice. The four time periods for start and runtime are annually, biannually, seasonally, and monthly. The second strategy was water-wise irrigation that used soil water deficit to schedule irrigation. The irrigation duration or the event runtime is based on the amount of water needed and was adjusted for the irrigation system's precipitation rate and efficiency.

Two types of irrigation system are specified: sprinklers for turf and ground covers, and drip irrigation for trees and shrubs.

The runtime RT (s) for each irrigation event is calculated based on

$$RT = \frac{PWR}{f_{irr}} \frac{1}{PR} \tag{1}$$

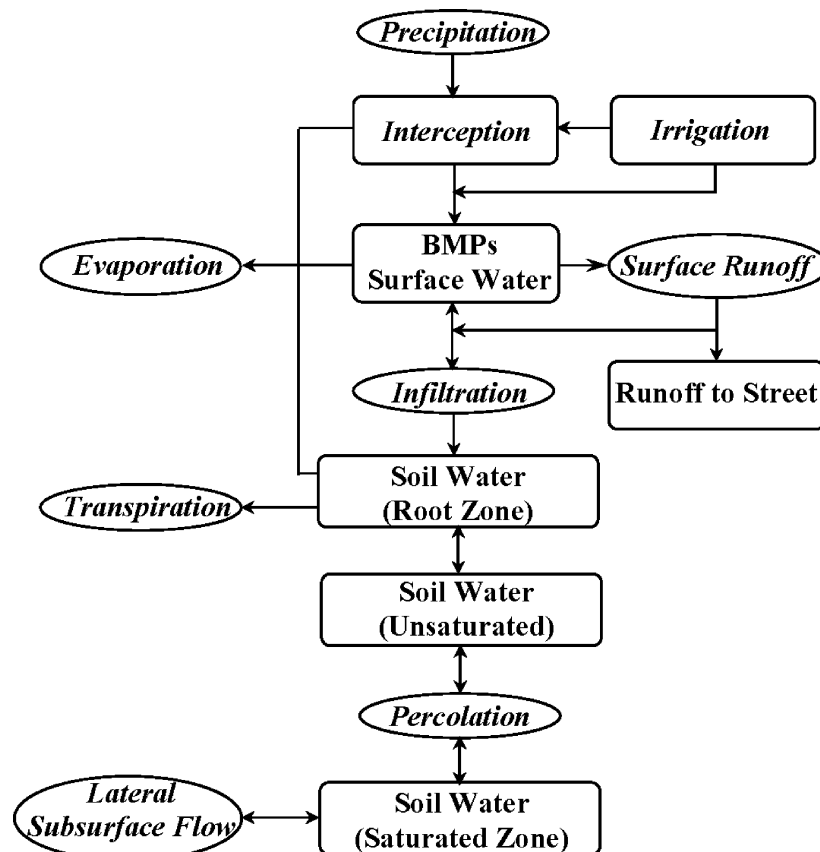


Figure 2. Model flow chart of hydrologic processes at the residential scale

where f_{irr} is the efficiency of the irrigation system. PR (m s^{-1}) is the precipitation rate of the irrigation system and PWR (m) is the plant's water requirements for that irrigation period, which is calculated as

$$\text{PWR} = \text{ET}_0 K_{\text{crop}} D \quad (2)$$

where ET_0 (m s^{-1}) is potential normal year evapotranspiration or historical reference ET. The crop coefficient K_{crop} is a dimensionless number ranging from 0.1 to 1.2 and depends on the characteristics of individual plant species (Costello *et al.*, 2000), and D (s) is the duration from the current irrigation event to the next irrigation.

For the soil water deficit irrigation scheduling, RT was calculated based on PWR and plant available water PAW (m) in the root zone RZ (m):

$$\begin{aligned} \text{PAW} &= \text{AW} \times \text{RZ} \\ \text{RT} &= \frac{(\text{PWR} - \text{PAW}) K_s}{f_{\text{irr}}} \frac{1}{\text{PR}} \end{aligned} \quad (3)$$

where AW (m) is available water in the root zone, which is determined by soil moisture and permanent wilting point. K_s is the stress factor. The depth of the RZ depends on both the plant species and the available soil depth.

Interception. Precipitation is intercepted by vegetation surfaces before it reaches the ground surface. The intercepted water will remain on the surfaces until it evaporates, drops off, or flows off the surface to reach ground surfaces (Xiao *et al.*, 1998). For vegetation interception, the governing equation used in this model is

$$\frac{dC}{dt} = p - f_g p - f_s p - d - e \quad (4)$$

where C (m) is canopy storage, t (s) is time, p (m s^{-1}) is precipitation rate, f_g is the fraction of free fall, f_s is the fraction of stem fall, d (m s^{-1}) is canopy drip rate, and e (m s^{-1}) is evaporation rate.

Canopy drip rate is described as an exponential function of canopy surface water storage and canopy water storage capacity. When canopy surface storage reaches capacity, drip begins:

$$d = d_0 e^{b(C-S)} \quad (5)$$

where S (m) is the canopy surface saturation storage capacity, d_0 (m s^{-1}) is the minimum drainage rate, which is the drainage rate when $C = S$, and b is a dimensionless parameter.

In natural hydrologic processes, canopy drip and evaporation occur before the full leaf surface gets wet. A wetting fraction f_{wet} is used for solving this partial wetting problem (Xiao *et al.*, 2000).

Evaporation e (m s^{-1}) of surface water is calculated by

$$\begin{aligned} e &= f_{\text{wet}} \text{ET}_0 \frac{C}{S} & C < S \\ e &= f_{\text{wet}} \text{ET}_0 & C \geq S \end{aligned} \quad (6)$$

where ET_0 (m s^{-1}) is potential evaporation rate at tree crown height (Xiao *et al.*, 1998). The calculation for ET_0 is described in detail in the 'Evapotranspiration' section.

Surface flow. Once the surface water storage depth exceeds its maximum capacity, surface flows begin. Because of both the shallow water storage depth and the relatively flat surface of the landscape, the surface flows are assumed as laminar flow. The governing equations for surface flow (Chow, 1959) in each land cover class are

$$v = \frac{1}{n} R^{2/3} S^{1/2} \quad (7)$$

$$\frac{dh}{dt} = p + q_{\text{in}} - f - e - q_{\text{out}}$$

where v (m s^{-1}) is the mean velocity in the cross-section, n is the Manning's roughness coefficient, R (m) is the hydraulic radius, S (m m^{-1}) is the slope, h (m) is surface water ponding depth, t (s) is time, p (m s^{-1}) is net precipitation rate, q_{in} (m s^{-1}) is surface flow into the model unit, f (m s^{-1}) is infiltration rate, e (m s^{-1}) is evaporation rate, and q_{out} (m s^{-1}) is surface flow out of the model unit. The hydraulic radius R is the same as the depth of surface water ponding depth h because of the overland flow.

The 1 h time interval could potentially cause problems in Equation (7) because, within this time-frame, water may flow across more than one land cover type. Using maximum surface velocity for time interval disaggregation (Ustin *et al.*, 1996) would increase the numerical accuracy. However, it also dramatically increases computation time as the slope of runoff course or the depth of water increases. Assuming that precipitation occurs at the beginning of the time interval, for steep modelling units ($>5^\circ$), such as roof surfaces (typically, a 26° roof slope for one-storey residential house), after surface runoff and evaporation, the surface water storage equals the surface detention storage. For a relatively flat surface, such as a driveway, Equation (7) was used directly because of the relatively small slope and shallow surface water storage depth.

Infiltration. Infiltration is the processes of surface water entry into the soil. It directly affects spatial and temporal dynamics of surface runoff and storage, as well as subsurface flow and storage. Water moving across a soil surface demonstrates loss in surface storage and gain in the vadose zone and or groundwater storage.

Infiltration processes are controlled by surface storage (water supply), subsurface moisture (potential water storage space) conditions, and soil hydrodynamic properties. Potential infiltration rates are estimated using the Green and Ampt equation (Green and Ampt, 1911):

$$f = K \left[1 + \frac{(\phi - \theta_i) S_f}{F} \right] \quad (8)$$

where f (m s^{-1}) is infiltration rate, K (m s^{-1}) is effective hydraulic conductivity, S_f (m) is the effective

suction at the wetting front, ϕ ($\text{m}^3 \text{m}^{-3}$) is soil porosity, θ_i ($\text{m}^3 \text{m}^{-3}$) is the initial water content, and F (m) is the cumulative infiltration.

Before any surface ponding occurs, infiltration rate is equal to the precipitation rate. After the surface ponding starts, the cumulative infiltration of the time period is calculated based on Equation (8) by using a forward finite-difference solution. The actual infiltration is adjusted for both surface and subsurface conditions.

Percolation. The percolation simulates flow through the root zone to the deep soil layer. The soil profile is stratified into four layers based on root zone depth of turf grass (0.61 m), shrub (1.22 m), tree (1.83 m), and deep soil layer (>1.83 m). Percolation of water in excess of field capacity from a layer is computed using (Savabi and Williams, 1995)

$$\begin{aligned} pe_i &= (\theta_i - FC_i)(1 - e^{-\Delta t/t_i}) & \theta_i > FC_i \\ pe_i &= 0 & \theta_i \leq FC_i \end{aligned} \quad (9)$$

where pe_i (m s^{-1}) is the percolation rate through layer i , FC_i is the field capacity of layer i , Δt (s) is the time interval, and t_i (s) is the travel time through layer i which is calculated with the linear storage equation:

$$t_i = \frac{\theta_i - FC_i}{K(\theta_i)} \quad (10)$$

where $K(\theta_i)$ (m s^{-1}) is the unsaturated hydraulic conductivity of layer i .

Unsaturated hydraulic conductivity is calculated according to the Van Genuchten (1980) and Mualem (1976) model:

$$\begin{aligned} K(S_e) &= K_0 S_e^L \{1 - [1 - S_e^{n/(n-1)}]^{(n-1)/n}\}^2 \\ S_e &= \frac{\theta - \theta_r}{\theta_s - \theta_r} \end{aligned} \quad (11)$$

where θ ($\text{m}^3 \text{m}^{-3}$) is soil water content, θ_r and θ_s ($\text{m}^3 \text{m}^{-3}$) are the residual and the saturated water contents respectively, S_e is the relative saturation, n is the curve shape parameter, which varies with soil type, L is an empirical pore tortuosity that is normally assumed to be 0.5 (Mualem, 1976), and K_0 (m s^{-1}) is the matching point at saturation.

Evapotranspiration. The process of evaporation occurs with all land cover types and vegetated surfaces as long as there is free water present at the surface. In contrast, transpiration only occurs with vegetation, and water is removed from the vadose zone.

Evaporation rate e (m s^{-1}) of surface water is described as

$$\begin{aligned} e &= ET_0 & S \geq S_{\min} \\ e &= \frac{S}{S_{\min}} ET_0 & S < S_{\min} \end{aligned} \quad (12)$$

where S and S_{\min} (m) are the surface water storage and the minimum storage depths respectively, and ET_0 (m

s^{-1}) is the potential evaporation rate, which is estimated using the modified Penman equation (Penman, 1948):

$$\begin{aligned} ET_0 &= wQ_{ne} + (1 - w)E_A \\ w &= \frac{\Delta}{\Delta + \gamma} \end{aligned} \quad (13)$$

where Δ is the rate of increase with temperature of the saturated water vapour pressure at air temperature, γ (Pa K^{-1}) is the psychrometric constant, Q_{ne} (m s^{-1}) is net radiation, and E_A (m s^{-1}) is the drying power of the air, which is defined as

$$E_A = c_e f_e(u_r)(e_a^* - e_a) \quad (14)$$

where e_a^* and e_a (Pa) are respectively the saturation vapour pressure and the vapour pressure at air temperature, c_e is a constant, and $f_e(u_r)$ is the wind function, described by (Pruitt and Doorenbos, 1977a,b)

$$f_e(u_r) = a_u + b_u u(z) \quad (15)$$

where a_u and b_u are constants and $u(z)$ (m s^{-1}) is the wind speed measured at height z (m) above ground surface.

We use the drying power of the air instead of aerodynamic resistance in Equation (14) to calculate potential evaporation because the wind function (Equation (15)) was well studied and used in CIMIS. Only four input parameters are needed for calculating ET_0 . These four parameters are net radiation, air temperature, wind speed, and vapour pressure.

The wind profile is retrieved from the wind speed measured at stand height (2.0 m from ground surface) at the meteorological station (Brutsaert, 1982; Jetten, 1996; Xiao *et al.*, 2000). We do not extrapolate air temperature and relative humidity from measurement height to actual canopy heights because the vertical gradient is small.

The plant transpiration rate T (m s^{-1}) is calculated based on potential evaporation rate ET_0 and plant crop coefficients K_{crop} . It is further adjusted by the moisture content of the root zone (Allen *et al.*, 1998):

$$\begin{aligned} T_p &= K_{\text{crop}} ET_0 \\ T &= \frac{\theta}{FC} T_p \end{aligned} \quad (16)$$

Lateral subsurface flow. Subsurface flow mass balance is described by

$$\frac{d\theta}{dt} = f + \sum q_{\text{in}} - \sum q_{\text{out}} - T - pe \quad (17)$$

where θ (m) is soil moisture, t (s) is time, f (m s^{-1}) is infiltration rate, q_{in} and q_{out} (m s^{-1}) are the water flow rates into and out of the problem domain, T (m s^{-1}) is the plant transpiration rate as defined in Equation (16), and pe (m s^{-1}) is the percolation rate to the deep soil layer or to the groundwater. Because of the relatively flat landscape and deep soil profile, we assumed that the subsurface water flow in and out of the problem domain is balanced.

Cistern water storage. Water storage change in the cistern is tracked from a simple mass balance equation:

$$\frac{dS}{dt} = Q_{in} - Q_{out} \quad (18)$$

where S (m^3) is the cistern storage, Q_{in} ($m^3 s^{-1}$) is the rate of water adding to the cistern, which is restricted by both the precipitation rate and the cistern collection area, and Q_{out} ($m^3 s^{-1}$) is the rate of water leaving the cistern that is discharged into the street, overflow or used for irrigation. Discharge cistern storage to the street occurs when the cistern is emptied before large storm events. For maximum BMP benefits, municipal water consumption on landscape irrigation begins when cistern reserves are depleted.

Initial and boundary conditions. All land cover surfaces are dry before precipitation or irrigation begins (Xiao *et al.*, 2000). Also, the soil water content of the vegetated area is at field capacity because of the routinely scheduled landscape irrigation.

Assume the landscape is sloped toward the street so that no surface water flows to or from adjacent parcels. Surface water flow can only travel to the street as surface runoff once it exceeds the storage capacities. Precipitation and irrigation occur at the top boundary where water enters the system. Evaporation and transpiration draw water out of the top boundary and into the atmosphere. At the bottom of the root zone, water percolates into the deep soil layer or into groundwater.

Input parameters. The model took explicit input information (dimensions and physical properties) on the location of the site, lot dimensions, soil, building, land cover types, trees, shrub masses, lawn, BMPs, and meteorological data. These values were measured from the field and laboratory or obtained from a nearby weather station. Trees in the parcel were treated as a BMP. Detailed physical properties and dimensions of each tree were derived from both field measurements and the tree growth curves described by Peper *et al.* (2001b). For the sensitivity analysis and retrofit simulation, we used a 'typical weather year' data. The typical weather year was defined

as the year in which its monthly precipitation and air temperature are close to the long-term (at least 10 years) averages. For simulating the system's response to storm events, precipitation data were selected based on historical rainfall data (e.g. NOAA weather station) and the depth–duration–frequency relations of the study area.

Output. For a typical weather year, the model simulation starts from current tree age and ends 40 years later. The results were presented at hourly, monthly, and annual scales. Monthly and annual output summarizes runoff discharged to the street, and landscape irrigation water use and water sources for irrigation.

For a storm event, the output included the dynamic change of runoff flow to the street, water storage of BMPs, and soil moisture content at an hourly time-scale. These data represent the storm runoff reduction by BMPs.

Other outputs included hourly soil moisture content and water storage of each unit.

Model calibration and validation. Data from the field measurement (control site) were used for model calibration and validation. During the field measurement period, no runoff discharge to the street was observed or measurable at the treatment site except the runoff from the sidewalk and the driveway outside the driveway interceptor. The runoff discharge to the street at the control site originated from the approximately half roof panel and driveway. Therefore, we used the soil moisture for calibration and validation of the model. Field data measured during the 2001–2002 rainy season were used for calibration. During the processes for calibration, soil moisture was set to the measured value as the initial condition. Soil moisture measured at 65 cm (25.6 in) deep was used to represent soil moisture at the tree root zone. By adjusting field capacity from 0.10 to 0.17, the soil water content at both field measurement sites and model output closely matched (Figure 3). The model was then tested against field data measured during the 2002 winter rain season for validation. The same pattern and good fit were found in the validation process, indicating that the calibration of input parameters was successful for these sites.

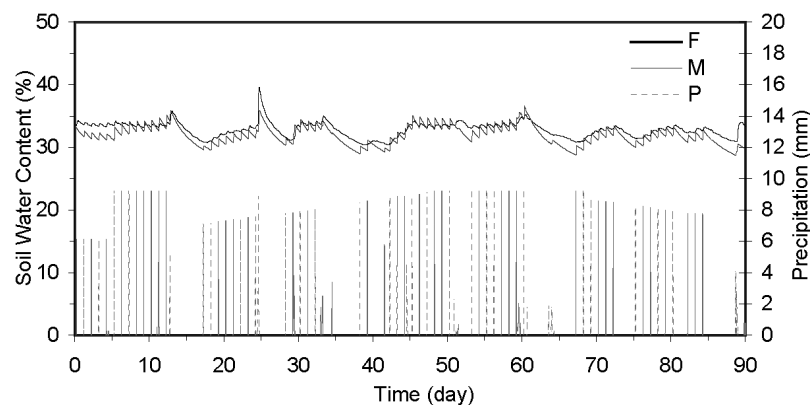


Figure 3. Soil moisture measured from the site (F) and from the model simulation (M). Precipitation (P) here included both rainfall and landscape irrigation

Numerical modelling. Numerical simulations were focused on annual landscape irrigation, annual and storm event runoff, evapotranspiration, and percolation to deep soil layers. Sensitivity analyses of landscape retrofit scenarios were simulated with two types of meteorological data.

We used 2001 meteorological data as the typical weather year meteorological data in the numerical simulation of annual runoff and landscape water use. In 2001, both monthly precipitation and temperature were close to the long-term (30 years) averages based on analysis of historical monthly precipitation and air temperature data (NOAA weather station at LAX, Coop ID: 045114; LAX is five miles southwest of the study site). Annual precipitation for 2001 at the study site was 426.0 mm (16.8 in). Figure 4 shows the temporal annual precipitation distribution. Of the 426 mm annual precipitation, 80% fell during the first 3 months. February was the wettest month, accounting for 44% of annual precipitation. The dry season started in May and extended to October or later.

For the 50-year rainfall event, we selected the 1 February 1998 storm based on an analysis of the historic meteorological data (NOAA weather station at LAX, Coop ID: 045114; 1948–2002 precipitation data) and the depth–duration–frequency relations of the study area (Tidemanson, 1991). This storm lasted 45 h with two separate events. The second event brought 78.2 mm (3.08 in) of the total 93.7 mm (3.69 in) precipitation.

To examine effects of BMPs on hydrological processes, a series of landscape retrofit scenarios was applied to the control site. The effects associated with each scenario were simulated.

Sensitivity analysis. The purpose of the sensitivity analysis was to distinguish which of the BMPs significantly influenced runoff reduction and conservation of landscape irrigation water use. There were no BMPs retrofitted at the control site, which served as the base condition. BMPs selected from the treatment site for evaluation were rain gutter, cistern, retention basin, drywell and driveway interceptor, and trees. The second analysis was conducted using clay soil because of the original site's sandy soil.

RESULTS

Field measurement

More than 50% of both parcels were covered by impervious surfaces. Buildings (house and garage) covered 35% of the treatment site and 31% of the control site. Driveways and walk paths covered 17% and 30% of the treatment and control sites respectively. Tree cover was 24% and 8% at the treatment and control site respectively. Turf grass covered 25% and 39% of the landscape at the treatment and control sites respectively. Analysis of field measurement data found BMPs (e.g. cistern and retention basins) to be effective in conserving municipal water supplies while maintaining an irrigated landscape, and reducing storm runoff. Surface runoff was effectively reduced through the installation of two BMPs: driveway interceptor and lawn retention basins. Sufficient soil moisture levels were maintained through the use of cistern reserves and municipally supplied water.

During 2 years of field measurements, there was no runoff discharge to the street from the lawn or from the front lawn retention basin at either site except from the driveway entrance area (3.4 m × 2.7 m (11.0 ft × 9.0 ft)) of the treatment site and from half of the roof and the entire driveway of the control site. The main reason for this result was that the annual precipitation and precipitation amounts for each storm event were relatively small. Rainfall rates did not exceed the soil infiltration rates measured at both sites. At the treatment site, the ratio of rainwater collection area (e.g. roof surface, lawn surface, partial of the driveway and other impervious paving area) to the rainwater receive area (e.g. the lawn area) was 2.04. The lawn retention basin could store a minimum (without infiltration and evaporation) of 30.4 m³ or maximum of 93.6 mm (3.7 in) of rainwater before it overflowed to the street. At the control site, this ratio is 1.41. Although the control site's lawn areas were not converted into a retention basin, the loamy sand soil in the lawn area was very permeable. The greatest storm event during 2001–2002 occurred on 10 February 2001 and lasted 92 h. This storm brought a total of 101.4 mm (3.99 in) rainwater. The maximum precipitation rate for this storm was 12.4 mm h⁻¹, which

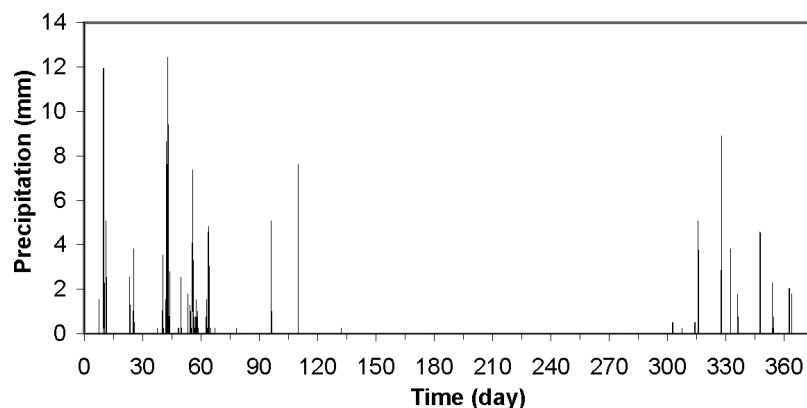


Figure 4. Annual precipitation for a typical weather year at the study site. Precipitation occurred during the wet winter rainy season. There was no rainfall during the dry summer season

was far below the infiltration rate of loamy sand soil (59.8 mm h^{-1}) (Maidment, 1993). The dynamic change of precipitation and soil water content at 35 cm depth is shown on Figure 5. The soil water content decreased quickly after peak rainfall.

Soil water content measured at the treatment site was higher than at the control site. Both sites had the same type of turf grass, but soil and radiation at these two sites were slightly different. The soil underneath the lawn retention basin in the treatment site had 5% higher soil bulk density than at the control site based on the field soil measurement. This suggested that the soil was compacted during the retrofit of the lawn area into a lawn retention basin. This compaction reduced the water conductivity of the soil. Two evergreen trees, a camphor tree (*Cinnamomum camphora*) with an 87.4 cm (34.4 in) diameter at breast height (DBH), and an avocado tree (*Persea americana*) with a 49.5 cm (19.5 in) DBH, were located on the west side of the treatment site. These two trees shaded large portions of the front and backyards, intercepted solar radiation and thus decreased the rate of ET for the treatment lawn relative to the control lawn.

The cistern installed in the treatment site has a maximum storage capacity of 11.4 m^3 (3000 gal) with a 38.7 m^2 (416.3 ft^2) rainwater collection area. The cistern was never entirely filled during the field measurement period due to the relatively small precipitation and water

collection area. However, the cistern still provided 3.7% of the annual water supply for landscape irrigation during our measurement period.

Numerical modelling

Sensitivity analysis. As expected, increased cistern storage provided additional water sources for irrigation. Cistern storage was affected by its collection area. Efficient use of the current cistern collection area increased cistern storage to 9.5% of annual water needed for landscape irrigation. Adding a rain gutter reduced runoff flow to street by 19.6%. Adding a rain gutter and a driveway interceptor reduced runoff to the street by 56%. Converting an existing lawn into a lawn retention basin reduced runoff to the street by 96.8%. Diverting water from the roof to the lawn reduced ET by only 3.3%, but it increased onsite water percolation. The combination of rain gutter, driveway interceptor, and lawn retention basin increased percolation by 37.6%. Similar results were found for an identical site, except with clay soil (Table II). For the 50-year flood event, a driveway interceptor was the most efficient BMP for storm runoff reduction. The driveway interceptor reduced annual runoff by 76.4%. Changing the lawn gradient or converting the lawn areas into retention basins reduced annual runoff to the street by only 12.3% (Table III). The rain gutter was less efficient for runoff reduction on clay soil because

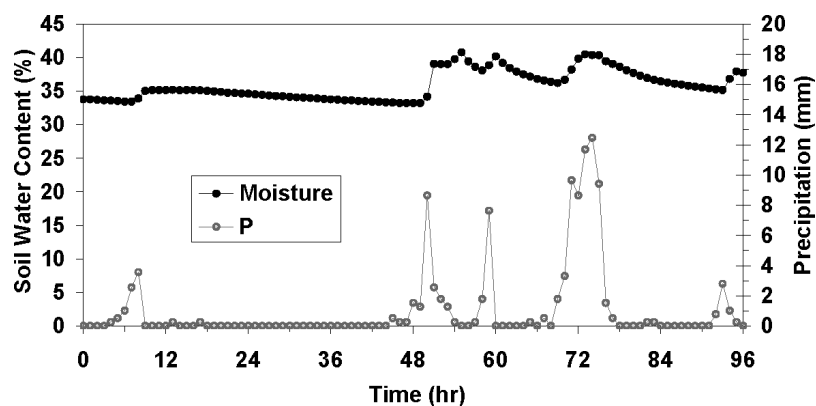


Figure 5. Dynamic soil water content during the 10 February 2001 storm event. The storm started at 4:00 am and lasted for 92 h. This storm consisted of three events and brought a total of 101.4 mm rainfall

Table II. Sensitivity analysis: runoff to street, evapotranspiration (ET), and percolation to groundwater (PGW) during a typical weather year

Treatment ^a	Sandy soil			Clay soil		
	Runoff %	ET %	PGW %	Runoff %	ET %	PGW %
Base	0.00	0.00	0.00	0.00	0.00	0.00
Rain Gutter (RG)	-19.60	-0.10	8.20	-11.70	-0.10	8.00
Cistern ^b	-21.30	-0.10	-2.00	-21.20	-0.10	-2.30
Lawn retention basin (LRB)	-33.40	3.40	7.40	-37.50	3.40	15.00
Driveway interceptor (DWI)	-56.00	0.00	23.20	-35.00	0.00	23.50
LRB and RG	-54.30	3.30	16.30	-57.20	3.30	28.70
LRB and DWI	-96.00	3.40	36.80	-95.30	3.40	60.70
LRB and RG and DWI	-96.80	3.30	37.60	-97.00	3.30	62.00

^a Total 296.8 m^3 precipitation for all treatments.

^b The cistern storage capacity is 11.4 m^3 (3,000 gal) with 106.2 m^2 rainwater collection area.

Table III. Sensitivity analysis: runoff reduction during a 50-year flood event

Treatments ^a	Sandy soil						Clay soil									
	Runoff to street			BMP storage			Runoff to street			BMP storage						
	Runoff	red. %	Cistern %	LRB %	Drywell %	VEGS %	Total	P ^b %	Runoff	red. %	Cistern %	LRB %	Drywell %	VEGS %	Total	P %
Base	27.7	0.0	0.0	0.0	0.0	100.0	2.4	3.6	41.2	0.0	0.0	0.0	0.0	100.0	2.4	3.6
Rain Gutter	20.1	-27.5	0.0	0.0	0.0	100.0	2.4	3.6	39.2	-4.9	0.0	0.0	0.0	100.0	2.4	3.6
Cistern	19.8	-28.7	80.6	0.0	0.0	19.4	12.2	18.6	31.9	-22.6	80.6	0.0	0.0	19.4	12.2	18.6
Lawn retention basin (LRB)	24.3	-12.3	0.0	53.8	0.0	46.2	2.5	3.9	24.3	-40.9	0.0	81.6	0.0	18.4	6.4	9.8
Driveway interceptor (DWI)	6.6	-76.4	0.0	0.0	0.6	99.4	2.4	3.6	33.8	-18.0	0.0	0.0	1.7	98.3	3.0	4.6
LRB and RG	1.8	-93.4	0.0	53.5	0.6	46.0	2.6	3.9	16.4	-95.6	0.0	95.6	0.2	4.2	28.2	43.2
LRB and DWI	16.4	-40.7	0.0	53.8	0.0	46.2	2.5	3.9	1.8	-60.1	0.0	91.0	0.0	9.0	13.1	20.1
LRB and RG and DWI	1.1	-95.9	0.0	53.5	0.6	46.0	2.6	3.9	1.1	-97.2	0.0	95.7	0.2	4.1	28.8	44.1

^a All treatments have a total 65.3 m³ precipitation.

^b % of total precipitation.

of the low infiltration rate, thus a lawn retention basin with rain gutter would be the single most efficient BMP for runoff reduction in this type of soil. The retention basin and driveway interceptor eliminated dry weather runoff flow to the street from the treatment site (Tables IV and V).

Landscape retrofits and best management practices.

Annual landscape irrigation water use varied widely depending on the irrigation controller setup. The setup also affected street runoff that was caused by splash and over-irrigation. Table IV shows the model simulation results for annual landscape irrigation water use and runoff flow to the street during 2001 for different irrigation controller setups. Table V shows monthly landscape irrigation water use and runoff flow to the street assuming a biannual irrigation controller setup. Model results suggested that water-wise irrigation could reduce landscape irrigation water use by 75.6% for the treatment site and 69.6% for the control site compared with the existing biannual irrigation schedule. After the cistern

Table IV. Annual landscape irrigation water use and runoff flow to the street

Setup ^a	Treatment site				Control site			
	TI ^b	IC	IM	R	TI	IC	IM	R
Fixed	520.0	15.3	504.7	3.8	483.8	0	483.8	157.6
Biannual	408.7	15.3	393.4	3.8	380.0	0	380.0	157.6
Seasonal	355.0	15.3	339.7	3.8	331.3	0	331.3	155.3
Monthly	270.9	15.0	255.9	3.8	253.1	0	253.1	148.4
Water-wise	126.8	14.1	112.7	3.8	147.1	0	147.1	144.5

^a Irrigation controller setup: fixed = no change; biannual = changes biannually; seasonal = changes seasonally; monthly = changes monthly; water-wise = changes depends on water demand.

^b Total landscape irrigation water use (TI), irrigation water from cistern storage (IC), irrigation water from municipal water supply (IM), and runoff (R) flow to street are in cubic meters.

Table V. Monthly landscape irrigation water use and runoff to street (biannual setup)

Month	P	Treatment site				Control site			
		TI	IC	IM	R	TI	IC	IM	R
1	82.8	26.7	4.4	22.3	1.1	24.8	0	24.8	38.4
2	129.2	23.9	6.8	17.1	1.7	21.2	0	21.2	58.9
3	22.1	25.1	1.2	23.9	0.3	23.0	0	23.0	12.3
4	19.5	43.0	1.0	42.0	0.2	40.1	0	40.1	10.9
5	0.2	42.8	0	42.8	0	40.1	0	40.1	2.4
6	0	42.8	0	42.8	0	40.1	0	40.1	2.4
7	0	42.8	0	42.8	0	40.1	0	40.1	2.4
8	0	46.1	0	46.1	0	43.1	0	43.1	2.6
9	0	39.5	0	39.5	0	37.0	0	37.0	2.2
10	0.7	26.4	0	26.4	0	24.8	0	24.8	2.7
11	23.7	24.9	1.1	23.8	0.3	23.0	0	23.0	12.0
12	18.6	24.8	0.8	24.0	0.2	23.0	0	23.0	10.2
Total	296.8	408.8	15.3	393.5	3.8	380.3	0	380.3	157.4

^a Total precipitation (P), total landscape irrigation water use (TI), irrigation water from cistern storage (IC), irrigation water from municipal water supply (IM), and runoff (R) flow to street are in cubic meters.

water reserve was depleted, the irrigation water resource was switched to city water. The cistern water storage provided 2.9–12.1% of total annual landscape irrigation water use for different irrigation setups. The dry weather runoff to the street was totally eliminated for the treatment site due to the conversion of the lawn into a lawn retention basin and driveway interceptor. In contrast, considerable runoff flowed from the control site to the street during the dry season due to overflows from landscape irrigation. The soil underneath the lawn is highly permeable; however, half of the lawn in the front yard was above ground level, and irrigation water drained to the driveway before infiltrating. Figure 6 shows the annual soil moisture dynamic change at both sites. The soil moisture was higher at the beginning and end of the year due to precipitation. During the summer season, the soil moisture had less variation due to irrigation.

For the 50-year storm event, the runoff flow to the street was 1.3% and 42.5% of total precipitation over the property at the treatment and control sites respectively (Figure 7a). At the treatment site, runoff flow to the street came from a small portion of the driveway (from the entrance to the driveway interceptor). In contrast, at the control site, the runoff flow to the street came from the entire driveway plus half of the roof. The BMP dynamic storage is shown in Figure 7b. As expected, water storage in the cistern increased as precipitation increased. The vegetated surfaces were saturated after the first event, but there was a storage peak at 38 h during this storm that was due to vegetation surface overstorage. Runoff from the roof was redirected to the lawn retention basin, which caused the rapid increase in water storage in the retention basin. The storage capacity of the retention basin was not reached. Storage in the swale (retention basin) was small because it only received precipitation. Surface runoff flowing to the swale retention basin only occurred when water over flowed from the lawn retention basin.

To examine the effects of BMPs on hydrologic processes, the control site was converted to a xeriscape landscape. Effects associated with each of the nine scenarios (change irrigation schedule, replace front yard turf with mulch and plant two trees, change the mulch area to swale retention basin, install rain gutter, install a driveway interceptor, replace 50% of backyard turf grass with mulch and plant two trees, change the backyard mulch area to a swale retention basin, and install a cistern) are presented in Table VI. The base case presented annual landscape water use and runoff for the existing control site's landscape.

There were two existing trees in the control site. A mature camphor (*C. camphora*) tree (>40 years old) was located in the front planting strip and an orange tree (*Citrus sinensis*, 15 years old) was located in the backyard. These trees' dimensions were changed annually based on growth data of the same tree species in southern California (Peper *et al.*, 2001a). Trees were planted to maintain or increase canopy coverage when the lawn

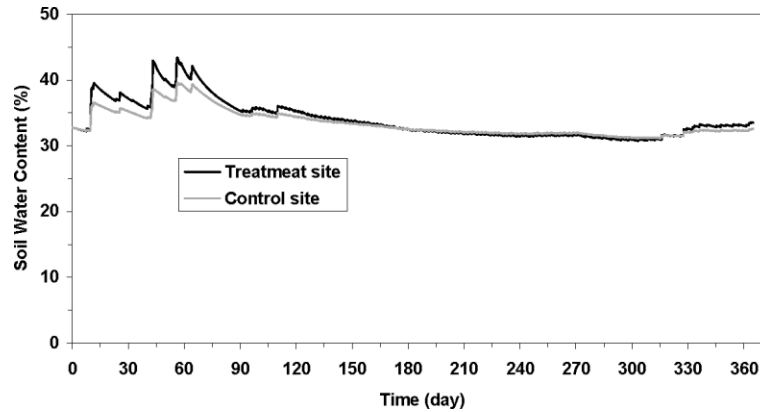


Figure 6. Dynamic soil water content for treatment and control sites. The higher water content in early months was due to the rainfall. About 79% of annual precipitation fell before 15 March

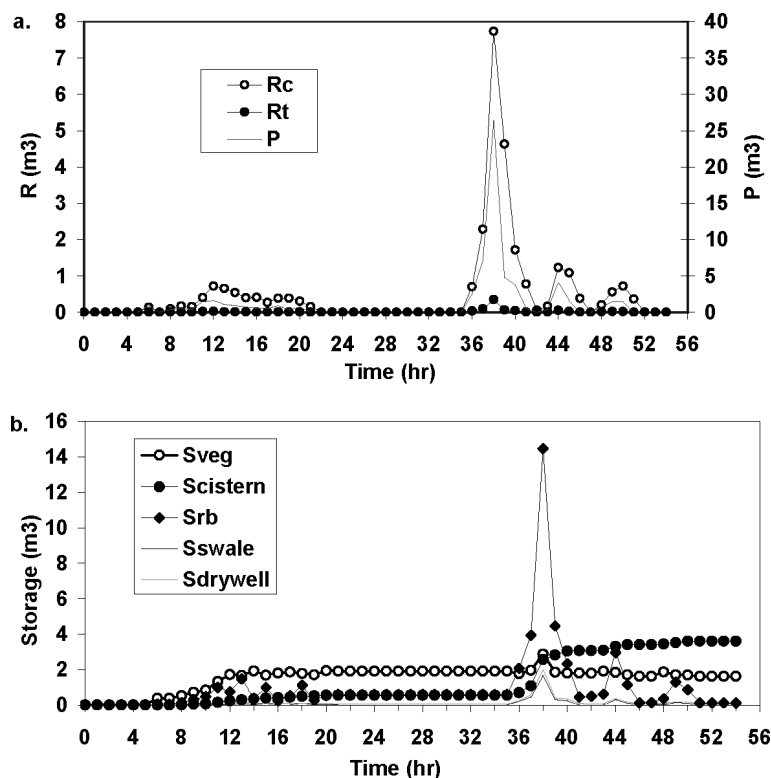


Figure 7. Runoff processes for a 50-year storm event. The storm started midnight on 1 February 1998. This storm lasted 45 h with two separate events and brought a total of 65.3 mm rainfall. (a) Precipitation P and runoff to the street for both treatment R_t and control R_c sites. (b) Surface retention storage dynamic change on the treatment site. Here S means storage. The S 's subscript denotes the BMP's name

area was converted into a retention basin. The evaluation was performed at 5-year intervals for a 40-year period. The total amount of runoff reduction increased as trees increased in size, as did water use. Changing the irrigation controller adjustment from the biannual (current practice) to monthly adjustment would reduce landscape irrigation water use to 86.6% and runoff to 95.8% compared with the base case. Further retrofits of the front yard lawn to mulch and planting two Coast live oak trees (*Quercus agrifolia*) would reduce landscape water use to 75.1% and runoff to 68.4%. Converting the mulched area into a detention basin did not change landscape irrigation water use or runoff to the street due to the precipitation rate and drip irrigation for

the trees. However, adding a rain gutter to allow roof runoff to flow to the retention basin reduced runoff to the street to 51.9%. Adding a driveway interceptor to redirect driveway runoff to the retention basin reduced runoff to 12.8%. Converting half of the backyard lawn into mulch and planting another two Coast live oak trees, converting the backyard mulch area into a detention basin, and installing an 11.4 m³ (3000 gal) cistern had no further effect on annual runoff flow to the street and landscape water use. However, water stored in the cistern provided 17.0–19.7% of annual landscape irrigation water demand.

We simulated annual runoff, canopy cover, and evapotranspiration change assuming that both the front and

Table VI. Landscape irrigation water use and runoff for landscape retrofit scenario of the control site

Landscape change ^a	Water use (%)					Runoff to street (%)				
	0 ^b	10	20	30	40	0	10	20	30	40
Base	100.0	102.4	103.9	103.9	103.9	100.0	99.3	98.9	98.9	98.9
Adjusting IC monthly (A)	85.6	89.1	90.5	90.5	90.5	95.8	95.0	94.6	94.6	94.6
(A) + replace FYT with munch and plant two trees (B)	75.1	82.8	92.2	101.0	106.7	68.4	68.2	64.7	61.4	58.9
(B) + SRB (C)	75.1	82.8	92.2	101.0	106.7	68.4	68.2	64.7	61.4	58.9
(C) + RG (D)	75.1	82.8	92.3	101.0	106.7	51.9	51.7	48.1	44.9	42.2
(D) + DWI (E)	75.2	82.9	92.4	101.1	106.8	12.8	12.8	12.5	12.2	12.0
(E) + replace 50% BYT with munch and plant two trees (F)	62.4	75.4	92.9	110.3	121.8	12.8	12.6	12.1	11.9	11.9
(F) + SRB (G)	62.4	75.3	92.9	110.3	121.7	12.8	12.6	12.1	11.9	11.9
(G) + cistern (H)	62.4	75.3	92.8	110.2	121.7	12.8	12.6	12.1	11.9	11.9
	19.7 ^c	19.9	20.1	18.7	17.0					

Landscape irrigation from cistern storage (%).

^a IC: irrigation controller; FYT: front yard turf; SRB: retention basin; RG: rain gutter; BYT: backyard turf.

^b Years after trees planted.

^c percentage landscape irrigation water use from cistern storage.

backyards of the control site were converted into retention basins but covered with rock mulch. Other BMPs included an 11.4 m³ (3000 gal) cistern, five Coast live oak trees (three in the front yard and two in the backyard), and a driveway interceptor. Figure 8 shows the change in annual runoff, canopy cover, and total evapotranspiration for this xeriscape retrofit. Canopy coverage gradually increased with age. The same pattern was found for evapotranspiration because ET was related to canopy cover. Runoff began to decrease 15 years after tree planting, reaching a 26% reduction at year 30. Annual runoff flow to the street decreased with tree age because rainwater interception increased with tree canopy coverage. Water consumption of each tree also increased with tree age. However, these big trees no longer need irrigation.

DISCUSSION

All BMPs installed at the treatment site were found to be effective management strategies for reducing storm runoff and irrigation demand from municipal water sources. The changes observed in the hydrologic regime were beneficial for the urban ecosystem. Reducing surface runoff not only decreased the potential storm runoff risk for the downstream reaches, but it also increased

deep percolation to groundwater. Compared with the base case (before retrofit), BMPs reduced the maximum runoff flow to the street by 96.8%, and maximum annual evaporation changed by 3.4%. Deep percolation increased by 37.6% for the sandy soil condition (Table II). The same pattern was observed for the clay soil condition. These results suggest that evapotranspiration changes at the site would not substantially alter the energy balance or enhance the urban heat island of urban landscapes such as this. In contrast, increased deep percolation would increase downstream base flow or groundwater recharge. These changes would benefit the urban ecosystem's hydrologic regime.

The driveway interceptor–drywell combination was the most efficient BMP for runoff reduction. However, this BMP may create a potential risk of transporting pollutants from the surface water to groundwater in areas with highly permeable soil. Applying treatment BMPs that could remove pollutants from the runoff before it enters the drywell could reduce this risk, especially in the early rainy season (Lee *et al.*, 2004). Further studies of BMPs, especially the effects of drywell percolation on groundwater contamination are needed before recommending large-scale application of BMPs.

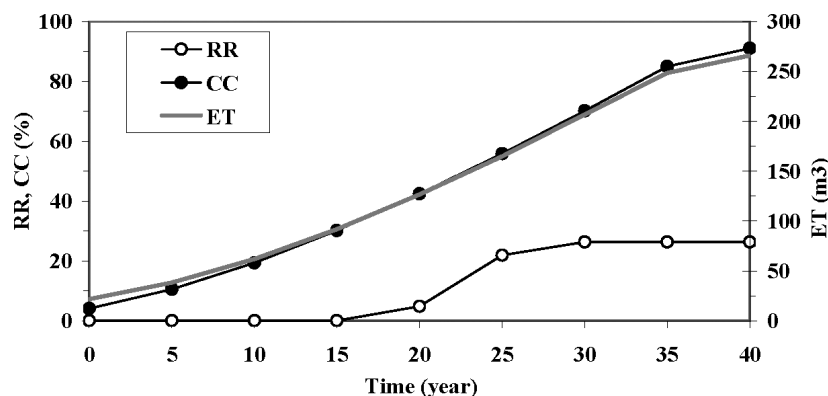


Figure 8. Annual runoff reduction (RR), evapotranspiration (ET), and canopy coverage (CC)

The cistern provides additional water sources for landscape irrigation. Filling the 11.4 m³ cistern provided 10% of annual landscape irrigation water demand. However, the cistern was not filled in the typical weather year due to an undersized catchment. Cistern benefits depend on appropriately sized catchment areas. Also, applying this BMP in climates with summer precipitation will allow the cistern to fill frequently.

This model was designed to work at the parcel scale. At this scale, hydrologic processes are affected by land cover change. The subsurface lateral inflow and outflow may not always be balanced for some landscapes, such as sites on steep hills or adjacent to water bodies. Thus, a more complex subsurface model is required for application in these topographic situations.

CONCLUSIONS

There is increased interest in controlling storm runoff at the source as an alternative to more centralized strategies. However, the ability of engineers and designers to evaluate the effectiveness of parcel-based BMPs has been hampered by the absence of tests on decision support tools. Moreover, models typically focus on runoff management, but not water harvesting and use for landscape irrigation. The numerical model described in this study can support better decision-making by allowing users to compare the effectiveness of different BMPs on parcels of any size and location. Using hourly meteorological data, simulation results can be obtained for a variety of storm events. Further testing and calibration are needed in different climate zones. Also, the model could be enhanced by incorporating lateral subsurface water flow and tracking the fate of different types of pollutant.

In this study's Los Angeles example, the driveway interceptor was the most effective BMP for storm runoff reduction (65%), followed by the rain gutter installation (28%), and lawn converted to retention basin (12%). An 11 m³ cistern did not substantially reduce runoff, but provided 9% of annual landscape irrigation demand. Annual landscape irrigation water use was reduced by 53% by increasing irrigation system efficiency and adjusting application rates based on plant water demand. Simulation results indicated that infiltration and surface runoff processes are particularly sensitive to the soil's physical properties and its effective depth. The implication is that soil testing is an important step in selecting the most appropriate BMP for any site.

ACKNOWLEDGEMENTS

We would like to express our appreciation to Steven Lennartz at the University of New Hampshire for his assistance with the fieldwork. We would also like to thank Rebecca Drayse and David O'Donnell at TreePeople of Los Angeles for their assistance with fieldwork and site mapping. This research was supported in part by funds provided by the Pacific Southwest Research Station of the

US Department of Agriculture Forest Service, and by the California Department of Forestry and Fire Protection.

REFERENCES

- Allen RG, Pereira LS, Raes D, Smith M. 1998. *Crop Evapotranspiration—Guidelines for Computing Crop Water Requirements*. FAO Irrigation and Drainage Paper 56. FAO: Rome.
- Bicknell BR, Imhoff JC, Kittle JLJ, Donigan ASJ, Johanson RC. 1997. *Hydrological Simulation Program-Fortran: user's manual for version 1*. EPA/600/R-97/080, US Environmental Protection Agency, National Exposure Research Laboratory, Athens, GA.
- Braune MJ, Wood A. 1999. Best management practices applied to urban runoff quantity and quality control. *Water Science and Technology* **39**(12): 117–121.
- Brutsaert W. 1982. *Evaporation into the Atmosphere. Theory, History, and Applications*. Environmental Fluid Mechanics. Kluwer: Dordrecht.
- Burian SJ, McPherson TN, Brown MJ, Streit GE, Turin HJ. 2002. Modeling the effects of air quality policy changes on water quality in urban areas. *Environmental Modeling & Assessment* **7**(3): 179–190.
- Chow VT. 1959. *Open-Channel Hydraulics*. McGraw-Hill: New York.
- Condon PM, Moriarty S, TreePeople. 1999. *Second nature adapting LA's landscape for sustainable living*. TreePeople, Beverly Hills, CA.
- Costello LR, Matheny NP, Clark JR, Jones KS. 2000. *A guide to estimating irrigation water needs of landscape plantings in California the landscape coefficient method and WUCOLS III. Estimating irrigation water needs of landscape plantings in California*. University of California Cooperative Extension, Sacramento.
- Gewe AG. 2003. *Water quality annual report*. Department of Water and Powe, Los Angeles, CA.
- Green WH, Ampt GA. 1911. Studies on soil physics: 1. Flow of air and water through soil. *Journal of Agricultural Science* **4**: 1–24.
- Grimmond CSB, Oke TR, Steyn DG. 1986. Urban water-balance. 1. A model for daily totals. *Water Resources Research* **22**(10): 1397–1403.
- Ha SR, Park SY, Park DH. 2003. Estimation of urban runoff and water quality using remote sensing and artificial intelligence. *Water Science and Technology* **47**(7–8): 319–325.
- Haile RW. 1996. *An epidemiological study of possible adverse health effects of swimming in Santa Monica Bay final report*. University of Southern California, CA.
- Haile RW, Witte JS, Gold M, Cressey R, McGee C, Millikan RC, Glasser A, Harawa N, Ervin C, Harmon P, Harper J, Dermand J, Alamillo J, Barrett K, Nides M, Wang GY. 1999. The health effects of swimming in ocean water contaminated by storm drain runoff. *Epidemiology* **10**(4): 355–363.
- Huber WC. 2001. New options for overland flow routing in SWMM, urban drainage modelling. *Proceedings, ASCE EWRI 2001 Conference*, Reston, VA: 22–29.
- Huber WC, Dickinson RE. 1988. *Storm water management model user's manual version 4*. EPA 600/3–88/001a. Environmental Research Laboratory, EPA, Athens, GA.
- Jetten VG. 1996. Interception of tropical rain forest: performance of a canopy water balance model. *Hydrological Processes* **10**: 671–685.
- Konrad CP, Burges SJ. 2001. Hydrologic mitigation using on-site residential storm-water detention. *Journal of Water Resources Planning and Management, ASCE* **127**(2): 99–107.
- LACSW Management (ed.). 2000. *A manual for the standard urban stormwater mitigation plan 2000*. Los Angeles County Department of Public Works, Environmental Programs Division, Alhambra, CA.
- Lee H, Lau SL, Kayhanian M, Stenstrom MK. 2004. Seasonal first flush phenomenon of urban stormwater discharges. *Water Research* **38**(19): 4153–4163.
- Lee JG, Heaney JP. 2003. Estimation of urban imperviousness and its impacts on storm water systems. *Journal of Water Resources Planning and Management, ASCE* **129**(5): 419–426.
- Maidment DR. 1993. *Handbook of Hydrology*. New York: McGraw-Hill.
- McPherson G, Simpson JR, Peper PJ, Maco SE, Xiao QF. 2005. Municipal forest benefits and costs in five US cities. *Journal of Forestry* **103**(8): 411–416.
- Metro. 2002. *Green streets: innovative solutions for stormwater and stream crossings*. Metro, c2002, Portland, OR.
- Mualem Y. 1976. A new model for predicting hydraulic conductivity of unsaturated porous-media. *Water Resources Research* **12**(3): 513–522.
- Penman KL. 1948. Natural evaporation from open water, bare soil, and grass. *Proceedings of the Royal Society of London, Series A: Mathematical and Physical Sciences* **198**: 116–140.

- Peper PJ, McPherson EG, Mori SM. 2001a. Equations for predicting diameter, height, crown width, and leaf area of San Joaquin Valley street trees. *Journal of Arboriculture* **27**(6): 306–317.
- Peper PJ, McPherson EG, Mori SM. 2001b. Predictive equations for dimensions and leaf area of coastal southern California street trees. *Journal of Arboriculture* **27**(4): 169–180.
- Pruitt WO, Doorenbos J. 1977a. Background and development of methods to predict reference crop evapotranspiration (ET₀). In *Crop Water Requirements. Irrigation and Drainage Paper No. 24*. FAO: Rome; 108–119.
- Pruitt WO, Doorenbos J. 1977b. Empirical calibration, a requisite for evapotranspiration formula based on daily or longer mean climate data. In *International Round Table Conference on 'Evapotranspiration'*, Budapest, Hungary. International Commission on Irrigation and Drainage; 20.
- Sanders LL. 1998. *A Manual of Field Hydrogeology. Field Hydrogeology*. Prentice Hall: Upper Saddle River, NJ.
- Savabi MR, Williams Jr. 1995. *Evaporation and environment*. WEPP model documentation. USDA–ARS National Soil Erosion Research Laboratory Publication.
- Stein ED, Tiefenthaler LL. 2005. Dry-weather metals and bacteria loading in an arid, urban watershed: Ballona Creek, California. *Water Air and Soil Pollution* **164**(1–4): 367–382.
- Thom RM, Borde AB, Richter KD, Hibler LF. 2001. Influence of urbanization on ecological processes in wetlands. In *Land Use and Watersheds: Human Influences on Hydrology and Geomorphology in Urban and Forest Areas*, Wigmoste MS, Borges SJ (eds). American Geophysical Union: Washington, DC; 5–16.
- Tidemanson TA. 1991. *Hydrology Manual*. In: L.A.C.D.o.P. Works (Editor), Los Angeles County Department of Public Works, 900 South Fremont Avenue, Alhambra, California 91803.
- Ustin SL, et al. 1996. *Modeling Terrestrial and Aquatic Ecosystem Responses to Hydrologic Regime in a California Watershed*, S. N. E. Project, editor. Sierra Nevada Ecosystem Project, Final Report to Congress: Assessments, Commissioned Reports, and Background Information. University of California, Centers for Water and Wildland Resources, Davis, CA; 275–308.
- Van Genuchten MT. 1980. A closed form equation for predicting the hydraulic conductivity of unsaturated soils. *Soil Science Society of America Journal* **44**(5): 892–898.
- Weng QH, Lu DS, Schubring J. 2004. Estimation of land surface temperature-vegetation abundance relationship for urban heat island studies. *Remote Sensing of Environment* **89**(4): 467–483.
- Wood MK, Jones TL, Vera-Cruz MT. 1998. Rainfall interception by selected plants in the Chihuahuan Desert. *Journal of Range Management* **51**(1): 91–96.
- Xiao Q, McPherson EG. 2002. Rainfall interception by Santa Monica's municipal urban forest. *Urban Ecosystems* **6**(4): 291–302.
- Xiao Q, McPherson EG, Simpson JR, Ustin SL. 1998. Rainfall interception by Sacramento's urban forest. *Journal of Arboriculture* **24**(4): 235–244.
- Xiao QF, McPherson EG, Ustin SL, Grismer ME. 2000. A new approach to modeling tree rainfall interception. *Journal of Geophysical Research–Atmospheres* **105**(D23): 29 173–29 188.